Delay and Delay-Constrained Throughput Analysis of a Wireless Powered Communication System

Zhidu Li†, Yuming Jiang‡, Yuehong Gao†, Lin Sang†, and Dacheng Yang†
†Wireless Theories and Technologies (WT&T) Lab, Beijing University of Posts and Telecommunications (BUPT), China
‡ Department of Telematics, Norwegian University of Science and Technology (NTNU), Norway

***Abstract*—In this paper, we investigate the delay and delay-constrained throughput performance of a point-to-point wireless-powered communication system, where one node, e.g. a user equipment (UE), is powered by the wireless energy transferred from the other node, e.g. an access point (AP), and uses the harvested wireless energy to send data to the other node. Our focus is on the delay performance of sending data over the uplink from the UE node to the AP node, and on its throughput performance when a delay constraint is enforced. Two representative time allocation schemes in using the link for the AP node to transfer energy (maybe together with data) and for the UE node to send data are considered. In particular, a lower bound on the cumulative capacity of the uplink is derived. In addition, an upper bound on the delay distribution is obtained for stochastic traffic arrivals, based on which, the delay-constrained throughput performance is further analyzed. Moreover, the accuracy of the analysis is validated by comparison with extensive simulation results. The analysis and results shed new light on the performance of such a wireless-powered communication system.**

I. Introduction

With the advance of wireless energy transfer technology, a newly emerging topic is wireless powered communication (WPC) [1] [2], which has recently attracted growing interest from both academia and industry. WPC has a great potential for use in a wide range of applications particularly in wireless sensor networks (WSNs) and Internet of Things/Everything (IoT/IoE) [2]. In a WPC system, a node, e.g. a user equipment (UE), harvests energy from the ambient radio signal, which may be purposely radiated by another node, e.g. an access point (AP), in its downlink (DL) to the UE node, and the UE node may then use the harvested energy to transmit data in the uplink (UL) to the AP node, as shown in Fig. 1.

Typically, in a WPC system, the UL and the DL share the same frequency band, which implies the system works in half-duplex mode. A fundamental issue of the WPC system is to decide how frequently the energy transfer should be conducted and how long each time the energy transfer should last. To provide answers to these questions, one has to investigate how much data needs to be sent by the UE node to the AP node, or equivalently what data throughput or capacity the system is intended to achieve. In addition, if there is delay requirement on the data, the investigation also should take it into account. These constitute the objective of this paper.

In the literature, several studies on the throughput performance of WPC systems can be found. In [3], the authors studied two types of throughput under a harvest-then-transmit protocol, which are the maximum system capacity and the throughput guaranteed for all devices at the same time. In [4], the focus was on spatial throughput maximization of a WPC network, by finding the optimal tradeoff between the energy transfer and information transfer. In [5], an optimization algorithm was proposed to maximize the system throughput in a multiuser multi-input-multi-output (MIMO) system through jointly optimizing the energy beamforming, receive beamforming and time slot allocation. In [6], under the requirement of a minimum throughput, the focus was on the energy efficiency through performing power control and time allocation jointly.

All these existing works [3]–[6] focus mostly on throughput studies with fluid traffic, where, delay, though a key performance metric, receives little attention. The-state-of-the-art study of delay performance in WPC systems is rather limited. Weakly related, in [7], a method to control the power-delay performance on demand in a WPC system was proposed, but its aim is to minimize the time-averaged power consumption with little touch on maximizing the throughput or capacity performance as in [3]–[6]. Actually, due to the limitation of hardware and energy transfer loss, the amount of harvested energy in a WPC system may be highly limited compared with the conventional systems powered through circuit [8]. Consequently, it is crucial to study the delay and throughput performance together for WPC systems.

In this paper, we investigate the delay and delay-constrained throughput performance of a point-to-point WPC system. Specifically, our focus is on the delay performance of sending data in the UL from the UE to the AP, and on its maximum throughput performance when a delay constraint is enforced. Two representative time allocation schemes to share the link for the AP to transfer energy and for the UE to send data are considered with one static and the other dynamic. A concise but tight lower bound is derived to characterize the complex cumulative service capacity process of the uplink under the two schemes. In addition, an upper bound on the delay distribution is obtained for stochastic traffic arrivals, based on which, the traffic delay performance and the delay-constrained throughput performance are further analyzed. It is found that, *when there is requirement on the delay performance, the consequent delay-constrained throughput performance under stochastic traffic may differ significantly from that under fluid traffic*. This sheds new light on the performance of WPC systems. Moreover, the accuracy of the analysis is validated by comparison with extensive simulation results.

The remainder is organized as follows. In Section II, the system model is presented. In Section III, detailed analysis of the WPC system is conducted. In Section IV, analytical and simulation results are presented, compared and discussed. Finally, we conclude the paper in Section V.

II. System Model

A. System Model

As shown in Fig. 1, we consider a point to point wireless powered communication system with an AP and a UE (e.g., a sensor). It is assumed that the AP and UE are equipped with one single antenna each. In the DL, the AP transfers wireless energy to the UE and the UE harvests the energy with a battery. In the UL, the harvested energy is used to send data from the UE to the AP. The DL and UL are assumed to share the same frequency band, i.e., the system works in half-duplex mode.

We focus on the data performance of the UE in the UL. The data traffic arrives at the UE randomly and is FIFO-served. A buffer is equipped at the UE to store the data packets that cannot be served immediately. The capacity of the battery and that of the buffer are assumed to be sufficiently large such that no battery overflow or buffer overflow would happen.

The time model consists of multiple consecutive time blocks (TBs) which are indexed by $1, 2, \cdots$. The time duration of each TB is fixed as T. The system adopts a harvest-then-transmit protocol, as depicted in Fig. 2. Specifically, in the ith TB, $i \in \mathbf{N}^*$ where $\mathbf{N}^*$ denotes the set of positive integers, the first $\tau_i T$ amount of time ($0 \leq \tau_i \leq 1$) is assigned to the AP to transfer wireless energy to the UE, while the remaining time $(1-\tau_i)T$ is assigned to the UE to send data to the AP as long as the UE is backlogged, i.e., having data to send. As used in the literature, we assume that the DL and UL channels are reciprocity and static with flat-fading, where in each TB, the complex channel gains of the DL and UL channels are both equal to a fixed value denoted by $\widetilde{h}$, i.e. the power gain is constant $h = |\widetilde{h}|^2$. In addition, we further assume that the channel state information (CSI) is perfectly known by the AP and UE at the beginning of each TB.

B. Data Transmission Capacity from UE to AP

Throughout this paper, the cumulative amount of traffic arrivals and that of the UE's data transmission service are expressed in the form of $Y(t)$ during time $[0, t)$ and $Y(s, t)$ during time $[s, t)$, i.e., $Y(s, t) = Y(t) - Y(s)$. Besides, the buffer and the battery are assumed to be empty at time 0.

The average transmission power of the AP, denoted by p_A, holds as $p_A = \mathbb{E}[|x_A|^2]$, where $\mathbb{E}[\cdot]$ is the expectation function and x_A is the radio signal. It is assumed that p_A is constant and sufficiently large over time, such that the wireless energy harvested due to the noise is negligible. Thus, the amount of energy harvested by the UE in the ith TB can be expressed as

$$P_i = \zeta p_A h \tau_i T,$$

where $0 < \zeta \leq 1$ is the energy harvesting efficiency. Further, since the traffic arrives randomly over time, energy may not be depleted in some TBs. Let E_i denote the amount of energy left at the beginning of the ith TB, there holds

$$E_{i+1} = E_i + P_i - p_i u_i, \tag{1}$$

where p_i and u_i denote the transmission power of the UE and the total transmission time in the ith TB respectively. Here, we assume, at the UE, its energy is mainly consumed by its data transmission, ignoring the other part of its functionalities.

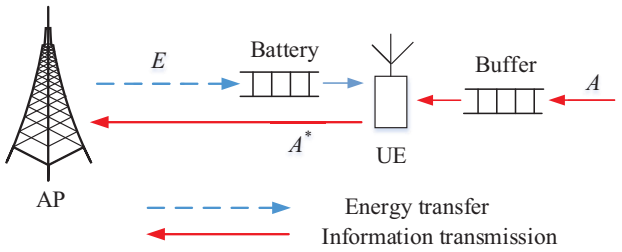

Fig. 1. System model with wireless energy transfer in the downlink and wireless information transmission in the uplink

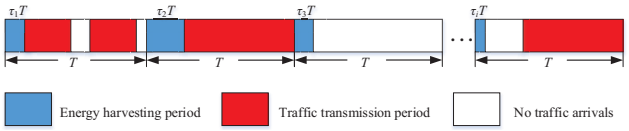

Fig. 2. The time (allocation) model

During the UL phase of the ith TB, the transmission rate of the UE holds as

$$R_i = W \log_2(1 + \frac{p_i h}{N_0 W}), \tag{2}$$

where N_0 denotes the power spectral density of background noise and W denotes the bandwidth.

The cumulative data transmission capacity of the UE from time s to time t, denoted by $C(s, t)$, can then be expressed as

$$C(s,t) = R_{\lceil \frac{s}{T} \rceil} \min\{(1-\tau_{\lceil \frac{s}{T} \rceil})T, \lceil \frac{s}{T} \rceil T - s)\} + \sum_{i=\lceil \frac{s}{T} \rceil + 1}^{\lfloor \frac{t}{T} \rfloor - 1} R_i(1-\tau_i)T + R_{\lfloor \frac{t}{T} \rfloor} \max\{t - \lfloor \frac{t}{T} \rfloor T - \tau_{\lfloor \frac{t}{T} \rfloor} T, 0\}. \tag{3}$$

C. Time Allocation

As indicated by (2) and (3), the data transmission service capacity of the UE is determined by the time allocation proportion $\{\tau_i : i \in \mathbf{N}^*\}$ and the transmission power at the UE $\{p_i : i \in \mathbf{N}^*\}$. In other words, the time allocation scheme for the AP to transfer wireless energy and for the UE to send data dominates the data transmission service capacity of the UE. We consider two time allocation schemes as follows.

Scheme 1. (**Static Time Allocation**) The time allocation proportion is fixed as τ_0 during the overall communications. The transmission power at the UE is determined as

$$p_i = \frac{E_i + P_i}{(1-\tau_0)T} = \frac{E_i + \zeta p_A h \tau_0 T}{(1-\tau_0)T}.$$

Scheme 2. (**Dynamic Time Allocation**) Choosing τ_i to maximize the cumulative service capacity $C((i-1)T, iT)$ in the ith TB, i.e.,

$$\max\{R_i(1-\tau_i)T\} = \max\{W \log_2(1 + \frac{p_i h}{N_0 W})(1-\tau_i)T\},$$

with the transmission power

$$p_i = \frac{E_i + P_i}{(1-\tau_i)T} = \frac{E_i + \zeta p_A h \tau_i T}{(1-\tau_i)T}.$$

The intuition behind Scheme 1 is to maximize the transmission power to use up the remaining energy and the harvested energy at the end of the TB, such that the total amount data that can be transmitted in this TB, or in other words the data transmission capacity in this TB, is maximized. In Scheme 2, with the same objective, it further exploits the potential of adapting τ_i, i.e., to find the optimal value for it through calculation at the beginning of each TB such that the data transmission capacity in this TB is maximized.

It is worth highlighting that the two schemes are intuitive and representative: They, particularly Scheme 2, are similar to the time allocation schemes in the existing works [3]–[6]. However, the analysis in [3]–[6] is limited to one TB only, which is therefore intractable to study the delay performance for stochastic traffic arrivals. Additionally, compared with Scheme 2, the communication in Scheme 1 only determines τ at the beginning of the first TB. Consequently, the calculation of Scheme 1 is far less than that of Scheme 2 in the long run.

D. Performance Metrics of Interest

We assume the traffic arrival process $A(t)$ to the UE is independent identically distributed (i.i.d). We use $A(s,t)$ to denote the cumulative amount of the traffic arrivals during time $[s,t)$. The departure process of $A(t)$ from the UL to the AP is denoted by $A^*(t)$. It is easily verified that, for such a system with input $A(t)$ and output $A^*(t)$, there holds [9]

$$A^*(t) = \inf_{0\le s\le t}\{A(s) + C(s,t)\}. \tag{4}$$

The objective of this paper is to study the delay and delay-constrained throughput performance for sending data from the UE to AP in the UL. The delay $D(t)$ is defined as [9]:

$$D(t) = \inf\{d : A(t) \le A^*(t+d)\}. \tag{5}$$

Note that $D(t)$ represents the delay of the last data packet arriving at t. If the arriving times of all packets are different, $D(t)$ is actually the real packet delay. The *delay-constrained throughput* is defined as the maximum traffic rate that the system can support for which the delay constraint is met [10]:

$$r_{\max} = \sup\{r : Pr\{D(t) > d\} \le \epsilon\}, \tag{6}$$

where r denotes the traffic arrival rate, and $Pr\{D(t) > d\} \le \epsilon$ the delay constraint, which says the probability that the delay exceeds the requirement d should not be higher than ϵ.

E. Remarks

In the system model described above, several assumptions have been made to simplify the analysis and the representation of the analytical results. They include: battery and buffer capacities are sufficiently large, harvested energy is mainly consumed by data transmission, the Shannon capacity is used as the (maximum achievable) data transmission rate, that there is no data loss, and the energy harvesting efficiency is constant. Here we provide some remarks on these assumptions.

First, many of these assumptions have been commonly adopted in the literature (see, e.g., [3]–[6]). Second, the analysis presented in this paper can be extended to cases where the assumptions are relaxed, which we leave as future work. Third, though these assumptions have led to simplified analysis, the analytical approach itself is not affected. In addition, the most appealing phenomenon, i.e., the delay-constrained throughput may significantly differ from the throughput without delay consideration, is sufficiently revealed by the obtained results, as later clearly seen from Fig. 6. Finally, we remark that the AP may transfer information to the UE together with the energy transfer in some WPC systems [11], and our analysis can be easily extended to study the data delay performance in the DL, but due to space limitation, we in this paper only focus on the data performance in the UL.

III. Performance Analysis

A. Bound on Cumulative Data Transmission Capacity

From (3), the form of the cumulative data transmission capacity is complex for application in performance analysis. The following theorem provides a lower bound on (3) to characterize the capacity which will be used in later analysis.

Theorem 1. *For any $t > 0$, the cumulative data transmission capacity in the time interval $[0,t)$ has a lower bound $\beta(t)$ regardless of using Scheme 1 or Scheme 2:*

$$\beta(t) = R_0(1-\tau_0)(t - \frac{\tau_0}{1-\tau_0}),$$

where $R_0 = W\log_2(1 + \frac{\zeta p_A h^2}{N_0 W}\frac{\tau_0}{1-\tau_0})$ and τ_0 is a fixed time allocation proportion over all the TBs.

Proof: Without loss of generality, we choose any one TB (indexed i) for analysis. Under Scheme 1, the cumulative capacity during the ith TB holds as

$$\begin{aligned} &W\log_2(1 + \frac{\frac{E_i + \zeta p_A h \tau_0 T}{(1-\tau_0)T}h}{N_0 W})(1-\tau_0)T \\ \ge &W\log_2(1 + \frac{\frac{\zeta p_A h \tau_0}{(1-\tau_0)}h}{N_0 W})(1-\tau_0)T \\ = &R_0(1-\tau_0)T \end{aligned}.$$

Under Scheme 2, since τ_i is the optimal value to maximize $R_i(1-\tau_i)T$. We have

$$\begin{aligned} &R_i(1-\tau_i)T \\ \ge &W\log_2(1 + \frac{\frac{E_i + \zeta p_A h \tau_0 T}{(1-\tau_0)T}}{N_0 W})(1-\tau_0)T \cdot \\ \ge &R_0(1-\tau_0)T \end{aligned}$$

From (3), for both two schemes, the following holds

$$\begin{aligned} C(t) &\ge R_0(\lfloor\frac{t}{T}\rfloor(1-\tau_0)T + \max\{t - \lfloor\frac{t}{T}\rfloor T - \tau_0 T, 0\}) \\ &\ge R_0(\lfloor\frac{t}{T}\rfloor(1-\tau_0)T + t - \lfloor\frac{t}{T}\rfloor T - \tau_0 T) \\ &\ge R_0(t - \tau_0 t - \tau_0 T) \\ &= R_0(1-\tau_0)(t - \frac{\tau_0}{1-\tau_0}) = \beta(t) \end{aligned}.$$

■

B. Delay Bound

The following theorem presents a delay bound for i.i.d traffic arrivals.

Theorem 2. *Consider a stable wireless powered communication system as depicted in Fig. 1, where the data transmission capacity of the UE is lower bounded by $\beta(t)$, and the traffic arrival process $A(t)$ is i.i.d distributed. Then the delay distribution of $D(t)$ is upper bounded by*

$$Pr\{D(t) > d\} \leq e^{-\theta(\inf_{0\leq s\leq t}\{\beta(s,t+d)-\alpha_\theta(s,t)\})},$$

for any $\theta > 0$ that is a free parameter and $\alpha_\theta(t) \geq \frac{1}{\theta}\log(\mathbb{E}[e^{\theta A(t)}])$ that denotes the statistical envelop of $A(t)$ [9] [12]*, where $\beta(s,t) \equiv \beta(t-s)$ and $\alpha_\theta(s,t) \equiv \alpha_\theta(t-s)$.*

Proof: Since event $\{D(t) > d\}$ implies event $A(t) > A^*(t+d)$, we have $\{D(t) > d\} \subseteq A(t) > A^*(t+d)$. Therefore [9],

$$\begin{aligned}
&Pr\{D(t) > d\}\\
\leq &Pr\{A(t) - A^*(t+d) > 0\}\\
\overset{(a)}{=} &Pr\{A(t) - \inf_{0\leq s\leq t+d}\{A(s) + C(s,t+d)\} > 0\}\\
\overset{(b)}{=} &Pr\{\sup_{0\leq s\leq t}\{A(s,t) - C(s,t+d)\} > 0\}\\
\overset{(c)}{\leq} &Pr\{\sup_{0\leq s\leq t}\{A(s,t) - \alpha_\theta(s,t) + \alpha_\theta(s,t) - \beta(s,t+d)\} > 0\}\\
\leq &Pr\{\sup_{0\leq s\leq t}\{A(s,t) - \alpha_\theta(s,t)\}\\
&> \inf_{0\leq s\leq t}\{\beta(s,t+d) - \alpha_\theta(s,t)\}\}
\end{aligned}$$

Here, step (a) is according to (4). In step (b), we adopt the time range $0 \leq s \leq t$ instead of $0 \leq s \leq t+d$ since if $s > t$, $A(t) < A^*(t+d)$. In step (c), we apply Theorem 1.

Let $V_s = e^{\theta(A(t-s,t)-\alpha_\theta(t-s,t))}$ and $X_k = A(k-1,k)$. Since $A(t)$ is i.i.d traffic, we have

$$\begin{aligned}
&\mathbb{E}[V_{s+1}|V_1, V_2, ...V_n]\\
=&\mathbb{E}[V_{s+1}|X_t, X_{t-1}, ...X_{t-s+1}]\\
=&\mathbb{E}[V_s e^{\theta(X_{t-s}-\alpha_\theta(t-s-1,t-s))}|X_t, X_{t-1}, ...X_{t-s+1}]\\
=&\mathbb{E}[V_s|X_t, X_{t-1}, ...X_{t-s+1}]\mathbb{E}[e^{\theta(X_{t-s}-\alpha_\theta(t-s-1,t-s))}]\\
=&V_s(\mathbb{E}[e^{\theta A(1)}] - \mathbb{E}[e^{\theta\alpha_\theta(1)}])\\
\leq &V_s
\end{aligned}$$

Hence, V_s is non-increasing with s. For the delay distribution, we have

$$\begin{aligned}
&Pr\{D(t) > d\}\\
\leq &Pr\{\sup_{1\leq s\leq t}\{V_{t-s}\} > \inf_{0\leq s\leq t}\{\beta(s,t+d) - \alpha_\theta(s,t)\}\}\\
= &Pr\{\sup_{1\leq m\leq t}\{V_m\} > \inf_{0\leq s\leq t}\{\beta(s,t+d) - \alpha_\theta(s,t)\}\}\\
\leq &Pr\{V_1 > \inf_{0\leq s\leq t}\{\beta(s,t+d) - \alpha_\theta(s,t)\}\}\\
\overset{(a)}{\leq} &e^{-\theta(\inf_{0\leq s\leq t}\{\beta(s,t+d)-\alpha_\theta(s,t)\})}(\mathbb{E}[e^{\theta A(1)}] - \mathbb{E}[e^{\theta\alpha_\theta(1)}])\\
\leq &e^{-\theta(\inf_{0\leq s\leq t}\{\beta(s,t+d)-\alpha_\theta(s,t)\})}
\end{aligned}$$

In step (a), we use the Chernoff bound. Therefore, Theorem 2 is proved. ■

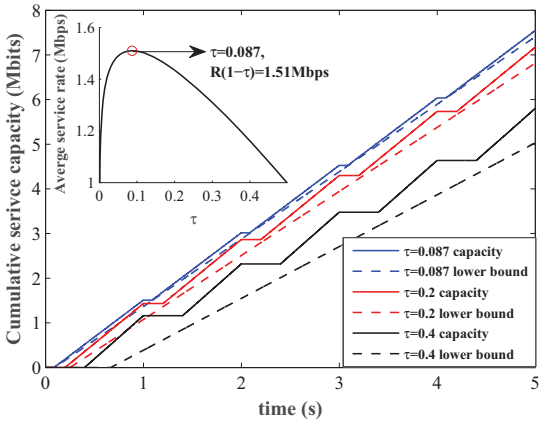

Fig. 3. Cumulative service capacity and service curve for different τ

As indicated by Theorem 2, the delay performance depends on both the cumulative capacity of the UL and the arrival traffic. In the rest of the paper, we consider two types of traffic for specific analysis.

Traffic 1. The arrival interval between two packets are exponentially distributed with parameter $1/\lambda$. The packet size L is assumed to be constant. The statistical envelop of Traffic 1 as introduced in Theorem 2 can be found as

$$\alpha_\theta(t) = \frac{1}{\theta}\log(\mathbb{E}[e^{\theta A(t)}]) = \frac{\lambda t}{\theta}(e^{\theta L} - 1). \tag{7}$$

Traffic 2. The traffic is fluid (i.e., the packet size is infinitesimal) with constant arrival rate $r_2 = \lambda L$.

According to Theorem 2, the delay distribution bound decreases with θ, i.e., a larger θ would achieve a tighter bound. However, θ should satisfy the following stability condition [9]

$$\lim_{t\to\infty}\frac{\alpha_\theta(t)}{t} \leq \lim_{t\to\infty}\frac{\beta(t)}{t}, \tag{8}$$

since otherwise the right hand of the delay bound in Theorem 2 would be larger than one, which is meaningless for probability.

Hence, for Traffic 1, the optimal θ can be found as

$$\theta_{opt} = \max\{\theta : \frac{\lambda}{\theta}(e^{\theta L} - 1) \leq R_0(1-\tau_0)\}. \tag{9}$$

Applying Theorem 2, the delay bound for Traffic 1 holds as

$$Pr\{D_1(t) > d\} \leq e^{-\theta_{opt}R_0(1-\tau_0)(d-\frac{\tau_0}{1-\tau_0}T)}. \tag{10}$$

Conversely, for constrained delay violation probability ϵ, the corresponding packet delay is bounded by

$$D_1(t) \leq -\frac{\ln\epsilon}{\theta_{opt}R_0(1-\tau_0)} + \frac{\tau_0}{1-\tau_0}T. \tag{11}$$

For Traffic 2, the arrival process is deterministic, based on which, the delay is always bounded as $D_2(t) \leq \tau_0 T$ on the condition that $r_2 \leq R_0(1-\tau_0)$ for system stability.

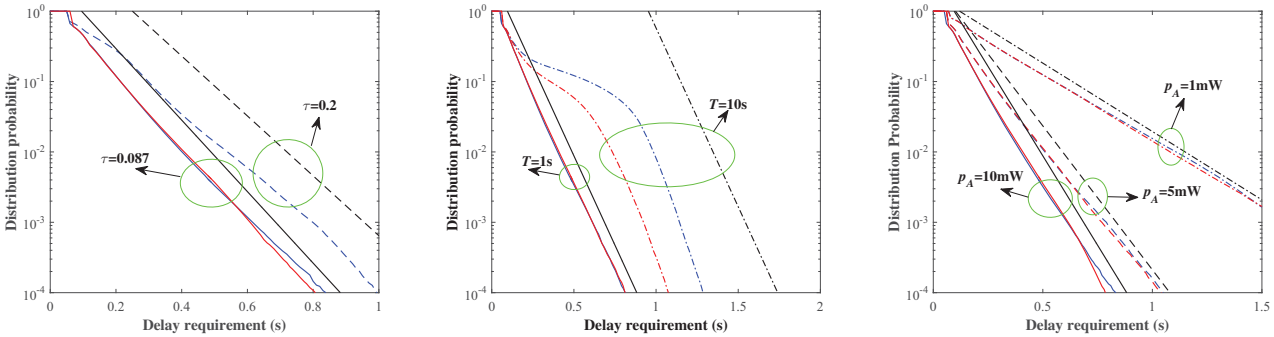

(a) Impact of τ (b) Impact of T (c) Impact of p_A

Fig. 4. Delay distribution under different parameters, where the blue line represents the simulation under Scheme 1, the red line represents the simulation under Scheme 2, the black line represents the analytical bound.

C. Delay-Constrained Throughput

In the following, we study the delay-constrained throughput defined in (6), and adopt τ_0 to be the solution of maximizing $\beta(t)$ obtained in Theorem 1 (see Fig. 3).

For deterministic traffic arrivals (Traffic 2), the delay-constrained throughput holds as

$$r_{\max,2} = R_0(1-\tau_0), \tag{12}$$

as long as the delay requirement $d \geq \tau_0 T$. Note that the obtained delay-constrained throughput agrees with the maximum throughput derived in [3] under one UE scenario. Interestingly, if the requirement is $d < \tau_0 T$, then the delay-constrained throughput is zero, i.e., the requirement cannot be met.

For stochastic traffic arrivals (Traffic 1), the delay constraint is represented by two parameters: the delay requirement $d \geq \frac{\tau_0}{1-\tau_0} T$ and the violation probability ϵ. With Theorem 2 and (8), the optimal θ can be solved from (9) as

$$\theta = -\frac{\ln \epsilon}{R_0(1-\tau_0)(d - \frac{\tau_0}{1-\tau_0})}.$$

In addition, according to the stability condition (8) and the expression of the statistical envelop of Traffic 2 in Theorem 2, the delay-constrained throughput holds as

$$r_{\max,1} = \lambda_{\max} L = \frac{R_0(1-\tau_0)\theta L}{e^{\theta L} - 1}. \tag{13}$$

It is worth highlighting that by loosening the delay constraint, the delay-constrained throughput under stochastic traffic converges to that of the fluid traffic, i.e.,

$$\lim_{\epsilon \to 1 \text{ and } d \to \infty} r_{\max,1} = R_0(1-\tau_0). \tag{14}$$

IV. Results

In this section, we present numerical results from the analysis and compare with simulation results. The adopted values of the various involved parameters are as follows: the bandwidth $W = 100$kHz, the power spectral density of the background noise $N_0 = -160$dBm, the channel power gain $h = 1$ and the energy harvesting efficiency ζ=1. Besides, without special statement, it is assumed that $p_A = 10$mW, $T = 1$s, $\tau = 0.087$, $\lambda = 10$ packets/s, $L = 100$kbits.

Fig. 3 depicts the cumulative capacity and the corresponding lower bound from Theorem 1, assuming that the traffic is saturated and the harvested energy is depleted in each TB. The sub-fig illustrates different τ would yield different average service rates, which exhibits an optimal point to maximize the average rate in one TB. In addition, the optimal τ minimizes the gap between the cumulative capacity and the lower bound. In other words, choosing optimal τ to allocation time for energy harvesting and data transmission improves not only the service capacity but also the accuracy of the lower bound.

In Fig. 4, the delay performance with Scheme 1 and Scheme 2 under Traffic 1 is depicted. The impacts of three system parameters are shown, i.e., τ, T and p_A. In each simulation experiment, 10^6 packets are generated. Scheme 1 and Scheme 2 are respectively applied to perform time allocation between energy harvesting and data transmission in each TB until all the packets are served. Each scheme is simulated for 10 times.

In Fig. 4(a), the delay performance is depicted with different τ. For Scheme 1 where τ is statically allocated, serving traffic with optimal τ achieves the best delay performance. Scheme 2, with dynamic adjustment of time allocation, is supposed to perform better than Scheme 1. Interestingly, the delay performance of Scheme 1 with optimal τ is actually close to that of Scheme 2. Additionally, the validity of the delay upper bound is also observed as expected from Theorem 2. Moreover, choosing optimal τ gains a significant improvement on the delay distribution bound for both schemes.

Fig. 4(b) depicts the impact of TB length T on the delay performance. The delay performance of Scheme 2 is remarkably better than Scheme 1 when T is large. However, as T decreases, the delay performance under both Scheme 1 and Scheme 2 is improved, and the performance difference between them becomes indistinguishable. In addition, the accuracy of the analytical bound is also significantly improved with reduced but more likely practical T. Specifically, when $T = 1$s, the analytical bound is tight. Actually, the parameter T cannot be too large in a practical system, since otherwise it would result in a high delay and need a large battery capacity to store the harvested energy.

Fig. 4(c) depicts the delay performance under different p_A. The delay performance is improved more significantly through

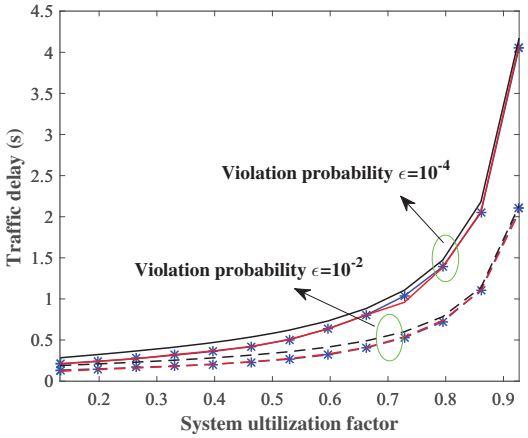

Fig. 5. Traffic delay for different delay violation probabilities, where the blue line represents the simulation under Scheme 1, the red line the simulation under Scheme 2, and the black line the analytical bound.

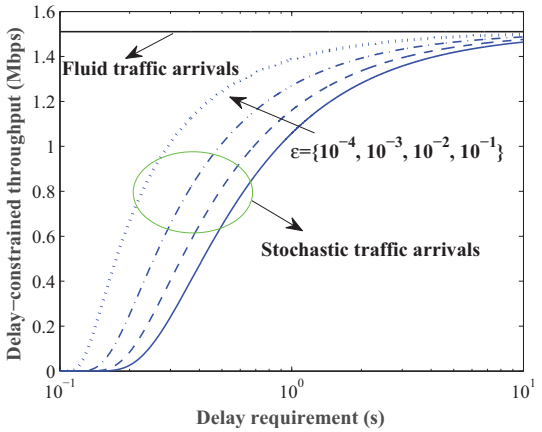

Fig. 6. Delay-constrained throughput

increasing p_A when p_A is low. Additionally, in all the three sub-figs of Fig. 4, all the simulation curves contain low delay points where the corresponding analytical curves cannot reach. This is because the packet arrival time is stochastic, which results in zero waiting time for some packets when the traffic load is not heavy. However, the analytical bound has a worst delay due to that it contains a time offset $\frac{\tau}{1-\tau}T$. Nevertheless, the validity of the analytical bound is observed from the figure.

In Fig. 5, the traffic delay is depicted as a function of system utilization defined as $\lambda L/R(1-\tau)$. The traffic delay under both Scheme 1 and Scheme 2 is illustrated. The figure shows that the analytical bound is tight, especially when the utilization is high. The reason is that the energy left at the end of each TB decreases as the utilization increases, which reduces the gap between the simulation and analytical results.

In Fig. 6, the delay-constrained throughput is depicted for different delay constraints. The maximum throughput with fluid traffic is independent of the delay constraint, which equals the system capacity for data transmission. Differently, the maximum throughput with stochastic traffic highly depends on both the delay requirement and the allowed delay violation probability. The higher delay or the higher delay violation probability the system can tolerate, the higher traffic rate the system can support or the higher throughput the traffic can acquire. Implied by the figure, with stochastic traffic arrivals, if there is delay requirement, using the capacity found from the fluid traffic model would easily lead to overestimation due to obvious gap between the capacity under fluid traffic and the delay-constrained throughput under stochastic traffic. This observation sheds new light on the performance of the system. However, when the delay constraint is loosened sufficiently, e.g., $d = 10, \epsilon = 0.1$, the delay-constrained throughput even with stochastic traffic arrivals converges to the conventional throughput without delay consideration under fluid traffic.

V. Conclusion

In this paper we presented an analytical approach to study the delay and delay-constrained throughput performance of a wireless powered communication system under two representative time allocation schemes: a static allocation scheme and a dynamic allocation scheme. Specifically, a lower bound on the cumulative data transmission capacity was first derived. In addition, based on the lower bound characterization of the capacity, an upper bound on the delay distribution was derived and elaborated with two types of traffic. Furthermore, the delay-constrained throughput was obtained for both types of traffic. The simulation results conform the validity and accuracy of the analytical results. The analysis and results shed new insights on the performance of a WPC system.

References

[1] S. Ulukus, A. Yener, E. Erkip, O. Simeone, M. Zorzi, P. Grover, and K. Huang, "Energy harvesting wireless communications: A review of recent advances," *IEEE J. Sel. Areas Commun.*, vol. 33, no. 3, 2015.

[2] S. Bi, C. K. Ho, and R. Zhang, "Wireless powered communication: opportunities and challenges," *IEEE Commun. Mag.*, vol. 53, no. 4, pp. 117–125, April 2015.

[3] H. Ju and R. Zhang, "Throughput maximization in wireless powered communication networks," *IEEE Trans. Wireless Commun.*, vol. 13, no. 1, pp. 418–428, January 2014.

[4] Y. L. Che, L. Duan, and R. Zhang, "Spatial throughput maximization of wireless powered communication networks," *IEEE J. Sel. Areas Commun.*, vol. 33, no. 8, pp. 1534–1548, Aug 2015.

[5] D. Hwang, D. I. Kim, and T. J. Lee, "Throughput maximization for multiuser MIMO wireless powered communication networks," *IEEE Trans. Veh. Technol.*, vol. 65, no. 7, pp. 5743–5748, July 2016.

[6] Q. Wu, M. Tao, D. W. K. Ng, W. Chen, and R. Schober, "Energy-efficient resource allocation for wireless powered communication networks," *IEEE Trans. Wireless Commun.*, vol. 15, no. 3, 2016.

[7] J. Yang, Q. Yang, K. S. Kwak, and R. R. Rao, "Power-delay tradeoff in wireless powered communication networks," *IEEE Trans. Veh. Technol.*, vol. PP, 2016.

[8] S. Kim and et al., "Ambient RF energy-harvesting technologies for self-sustainable standalone wireless sensor platforms," *Proc. of the IEEE*, vol. 102, no. 11, pp. 1649–1666, Nov 2014.

[9] Y. Jiang and Y. Liu, *Stochastic Network Calculus*. Springer, 2008.

[10] Y. Gao and Y. Jiang, "Analysis on the capacity of a cognitive radio network under delay constraints," *IEICE Trans. Commun.*, vol. E95-B, no. 4, 2012.

[11] X. Zhou, R. Zhang, and C. K. Ho, "Wireless information and power transfer: Architecture design and rate-energy tradeoff," *IEEE Trans. Commun.*, vol. 61, no. 11, pp. 4754–4767, November 2013.

[12] C. Li, A. Burchard, and J. Liebeherr, "A network calculus with effective bandwidth," *IEEE/ACM Trans. on Netw.*, vol. 15, no. 6, 2007.